Electronic Supplementary Information for Tunable, Shape-shifting Capsule for Dicarboxylates

*Qi-Qiang Wang, Victor W. Day, and Kristin Bowman-James**

Department of Chemistry, University of Kansas, Lawrence, Kansas 66045

*E-mail: kbjames@ku.edu

Contents

Synthesis and characterization of the tricyclic host 1

7.3 g (50 mmol) of tris(2-aminoethyl)amine and 14.6 g (75 mmol) of dimethyl 2, 6-pyridinedicarboxylate were dissolved in 1500 mL methanol and heated at reflux for two weeks. Then the reaction mixture was concentrated to remove the solvent and subjected to column chromatography on basic aluminum oxide (~150 mesh, gradient elution 2% v. CH_3OH in CH_2Cl_2 to 7% v. CH_3OH in CH_2Cl_2) to give 0.45 g (3%) **1** and 1.63 g (10%) of a bicyclic cryptand as white solids after recrystallization in methanol. **1**: δ_H (400 MHz, DMSO-d_6) 9.23 (t, J = 6.2 Hz, 4H), 8.73 (t, J = 5.4 Hz, 8H), 8.03-7.87 (m, 18H), 3.44 (q, J = 6.4 Hz, 8H), 3.34 (q, J = 5.8 Hz, 16H), 2.78 (t, J = 5.8 Hz, 16H), 2.74 (t, J = 6.4 Hz, 8H); δ_C (125 MHz, $CDCl_3$) 164.1, 148.9, 139.4, 139.2, 125.2, 60.0, 58.5, 40.8, 40.0; Exact mass for $C_{66}H_{78}N_{22}O_{12} + H^+$ 1371.6248, found 1371.6219.

NMR studies

^{1}H NMR spectra were recorded on a Bruker Avance 400 spectrometer at 400 MHz. Each titration was performed by 20 measurements in DMSO-d_6 at room temperature. Aliquots from a stock solution of the nBu$_4$N$^+$ salts (20 mM) were gradually added to the initial solution of ligand (2 mM). Up to ten anion equivalents were added during the titrations. All proton signals were referenced to a TMS standard. For fast exchange process, the association constants K were calculated by EQNMR. All titration curves fit best in 1:1 binding modes of the ligand to anions. The total concentration of the ligand and anion was 2 mM for Job plot analysis.

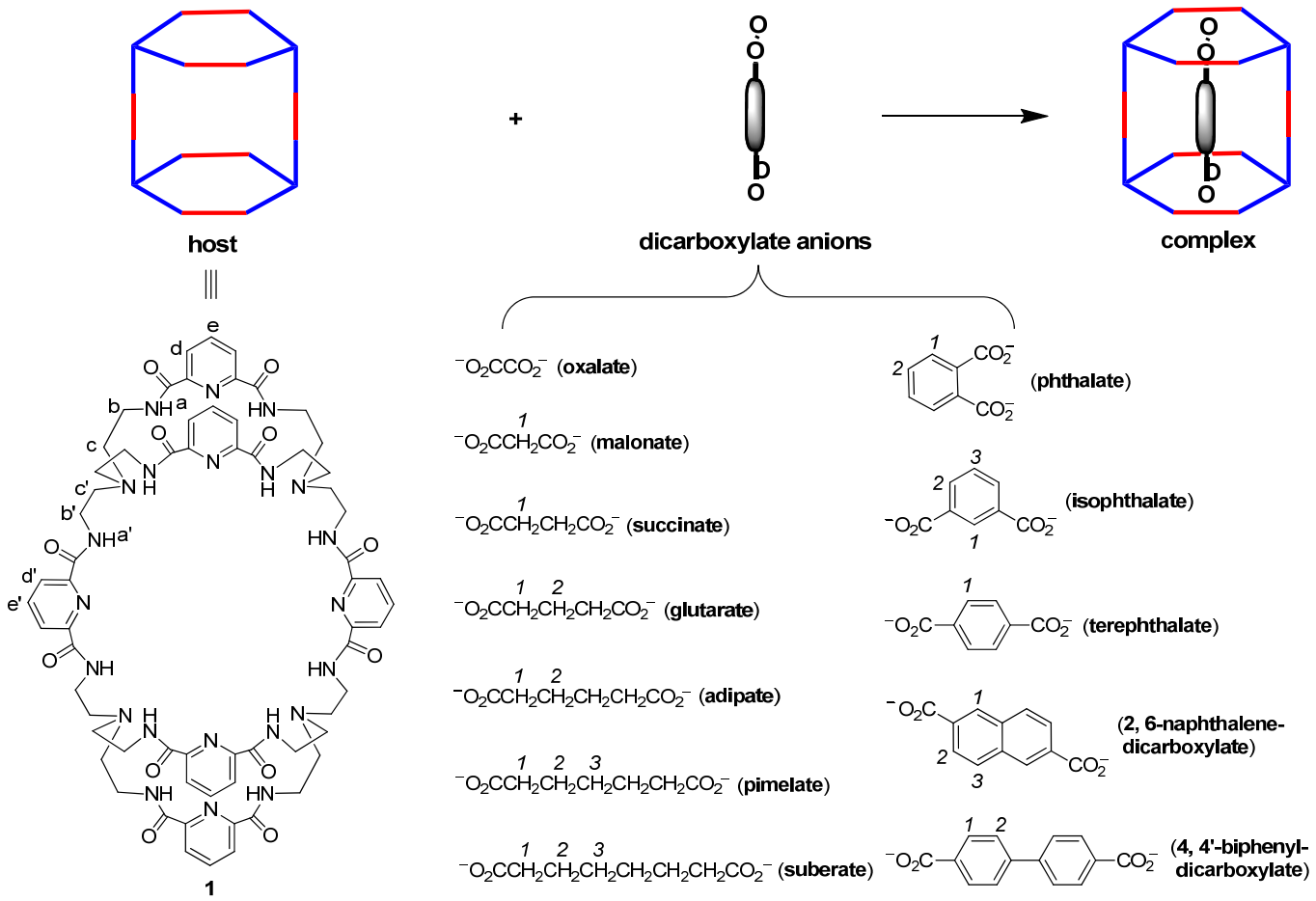

Figure S1. ChemDraw diagrams of **1** and dicarboxylates showing labeling of protons for NMR data.

Table **S1.** The chemical shift changes between the complexes and the free host, dicarboxylates upon encapsulation.

Dicarboxylates	$\delta_{complex}$- δ_{host} (ppm)					$\delta_{complex}$- $\delta_{dicarboxylate}$ (ppm)
	NH^a	$NH^{a'}$	$(CH_2)^{b'}$	$(CH_2)^c$	$(CH_2)^{c'}$	
oxalate	[a]	[a]	[a]	[a]	[a]	
malonate	[a]	[a]	[a]	[a]	[a]	[a]
succinate	+1.57	+0.08	[a]	[a]	[a]	*1*: > +0.7
glutarate	+1.54	+0.24	[a]	−0.11	−0.01	*1*: +0.5 ~ +0.6; *2*: +0.48
adipate	+1.59	+0.24	[a]	−0.09	−0.04	*1*: +0.27; *2*: +0.2 ~ +0.3
pimelate	+1.53	+0.27	[a]	−0.11	−0.07	*1*: +0.40; *2*: +0.1 ~ +0.2; *3*: +0.2 ~ +0.3
suberate	+1.57	+0.28	[a]	−0.12	−0.07	*1*: +0.34; *2*: +0.05 ~ +0.14; *3*: +0.04
phthalate	[a]	[a]	[a]	−0.16	−0.03	*1*: +0.34; *2*: +0.02
isophthalate[b]	+1.65	+0.11	[a]	[a]	[a]	*1*: +0.87; *2*: +0.25; *3*: −0.16
terephthalate	+1.67	−0.03	−0.43	−0.17	−0.12	*1*: +0.17
2, 6-naphthalene	+1.82	−0.31	−0.19	−0.32	−0.27	*1*: +0.19; *2*: +0.04; *3*: −0.81
4, 4'-biphenyl[c]	+1.80	−0.19	−0.19	−0.31	−0.37	*1*: ~ +0.3; *2*: ~ +0.2

[a] The value was not shown due to the peak broadening or illegibility. [b] The average value for the two unequivalent NH^a (+1.80, +1.49 ppm). [c] The value was estimated due to the fast exchange process on NMR scale between the host, dicarboxylate and the complex.

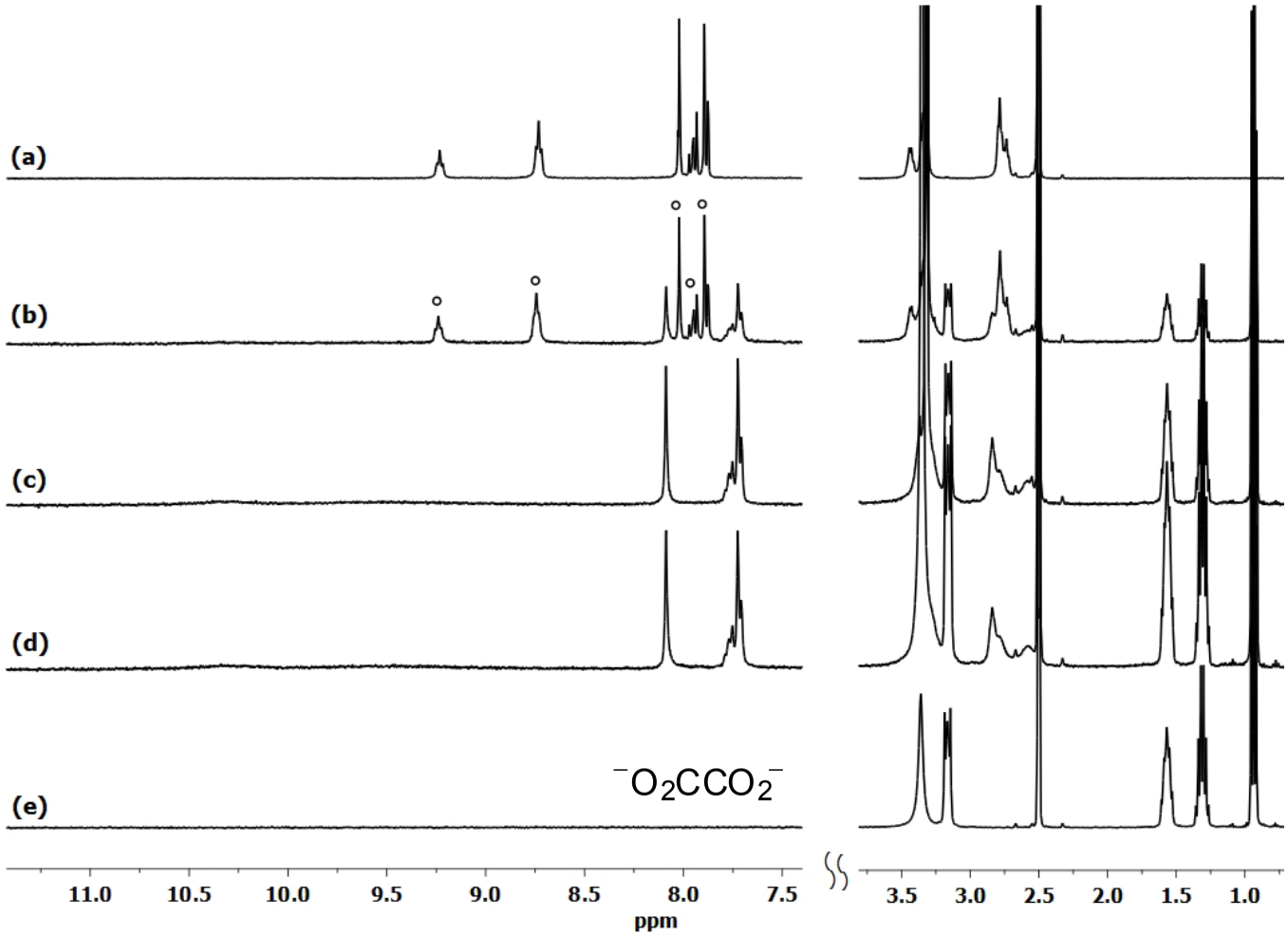

Figure S2. ^{1}H NMR spectra of **1** in DMSO-d_6 after adding oxalate in different ratios (**1**/oxalate): (a) 1:0, (b) 1:0.5, (c) 1:1, (d) 1:2 and (e) 0:1. The amide NH broadened upon binding. "◦" correspond to the signals of the unbound host.

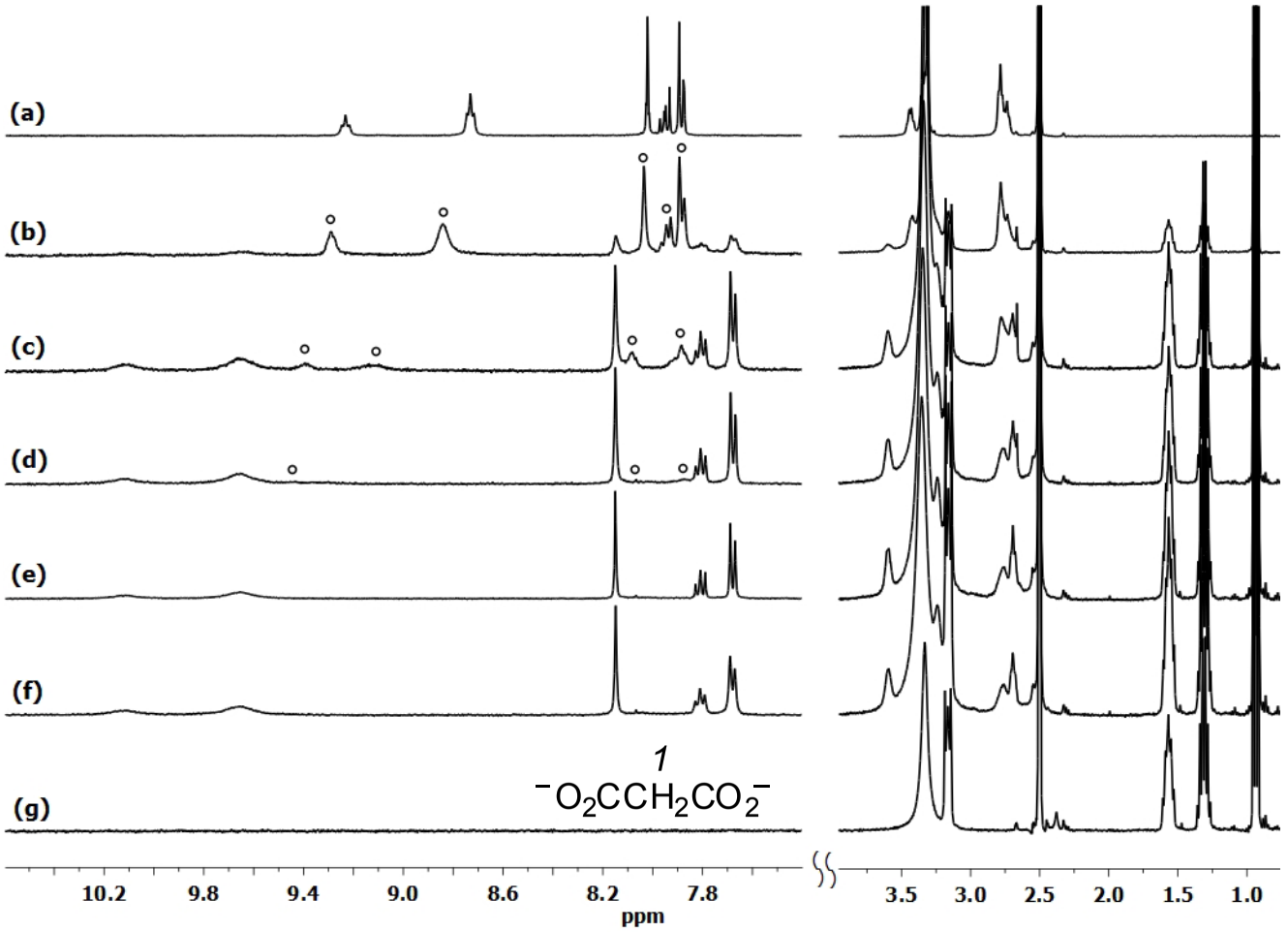

Figure S3. ^{1}H NMR spectra of **1** in DMSO-d_6 after adding malonate in different ratios (**1**/malonate): (a) 1:0, (b) 1:0.5, (c) 1:1, (d) 1:1.3, (e) 1:1.6, (f) 1:2 and (g) 0:1. "∘" correspond to the signals of the unbound host.

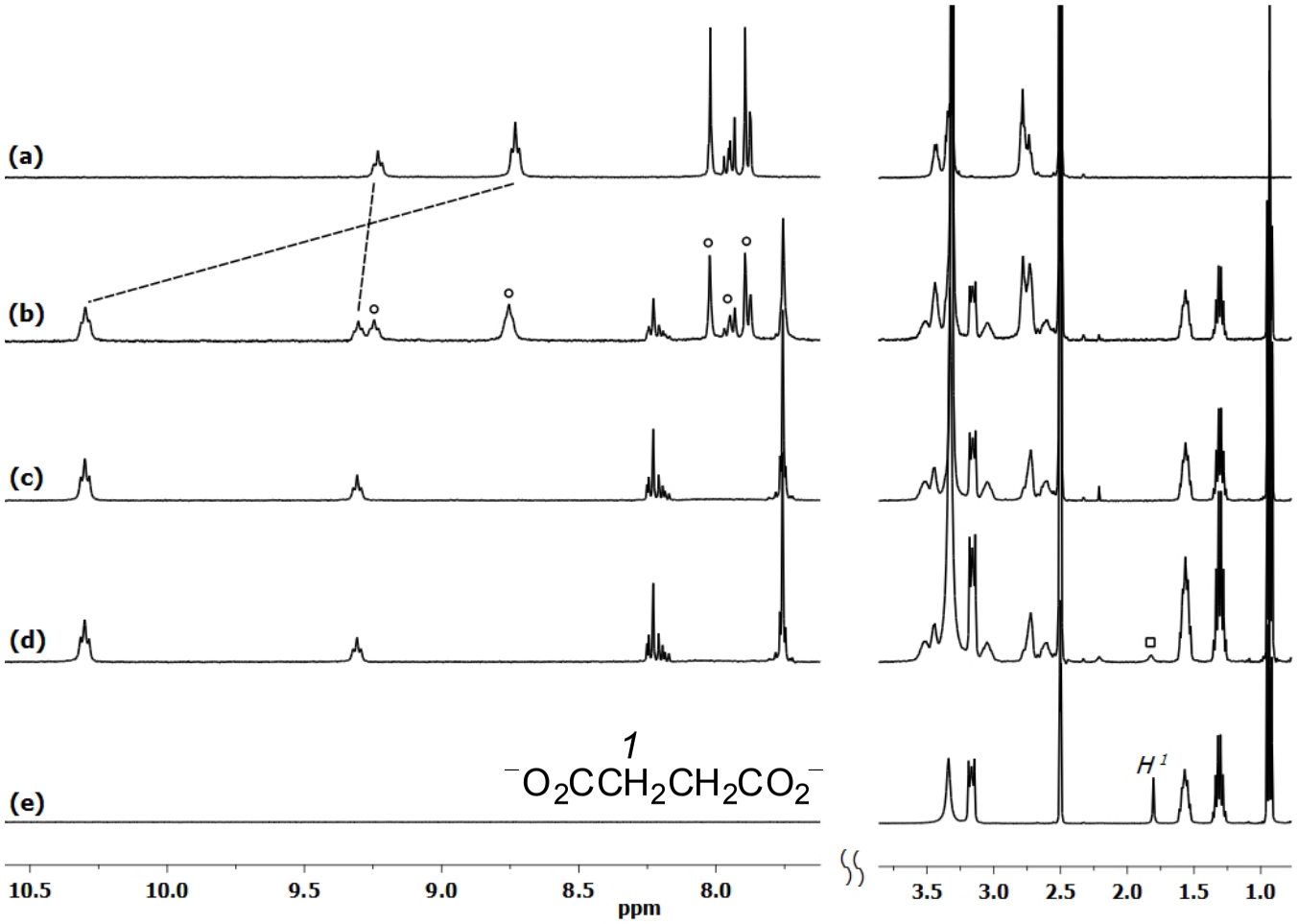

Figure S4. ^{1}H NMR spectra of **1** in DMSO-d_6 after adding succinate in different ratios (**1**/succinate): (a) 1:0, (b) 1:0.5, (c) 1:1, (d) 1:2 and (e) 0:1. "◦" and "▫" correspond to the signals of the unbound host and dicarboxylate respectively.

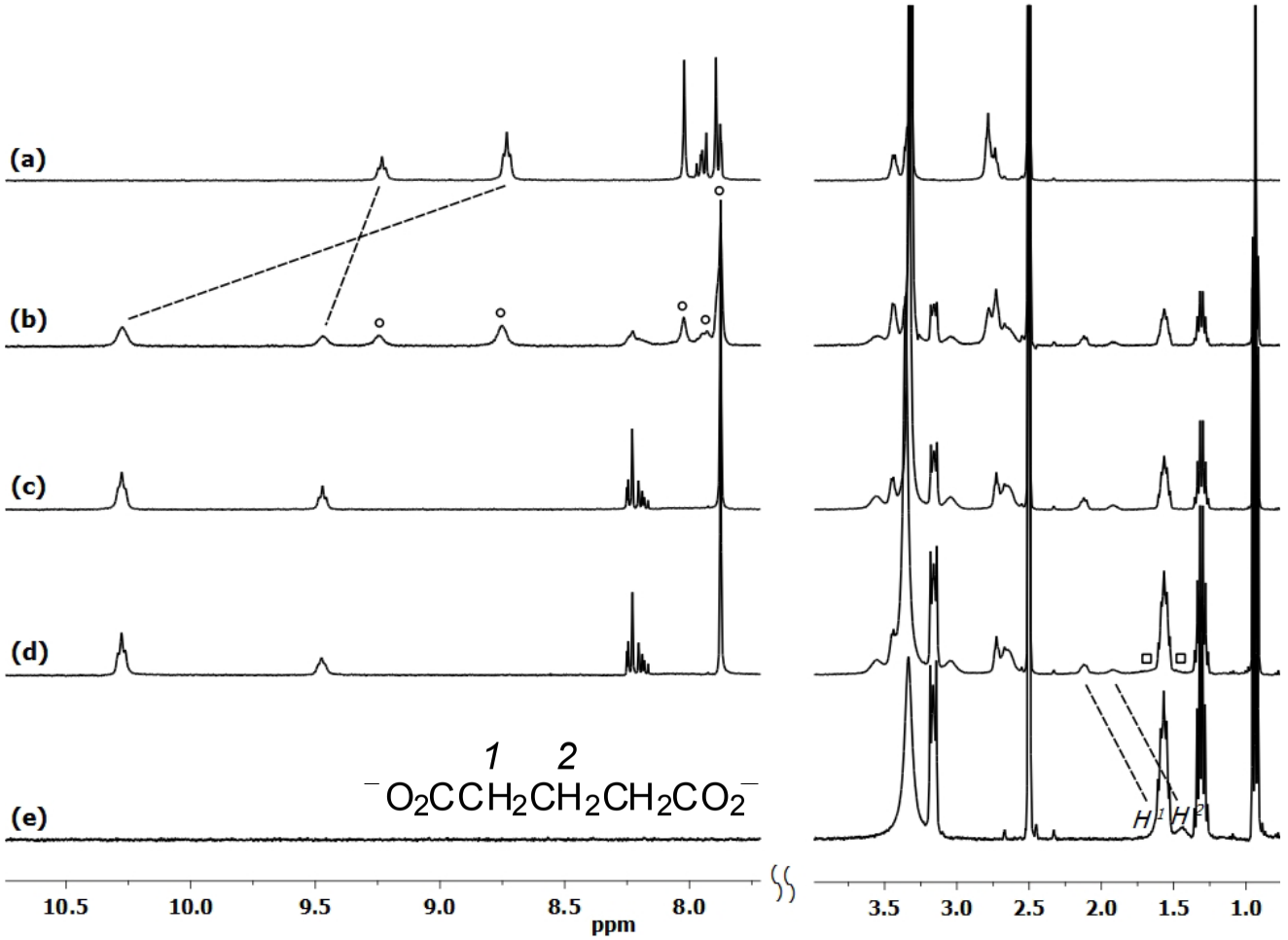

Figure S5. ^{1}H NMR spectra of **1** in DMSO-d_6 after adding glutarate in different ratios (**1**/glutarate): (a) 1:0, (b) 1:0.5, (c) 1:1, (d) 1:2 and (e) 0:1. "◦" and "▫" correspond to the signals of the unbound host and dicarboxylate respectively.

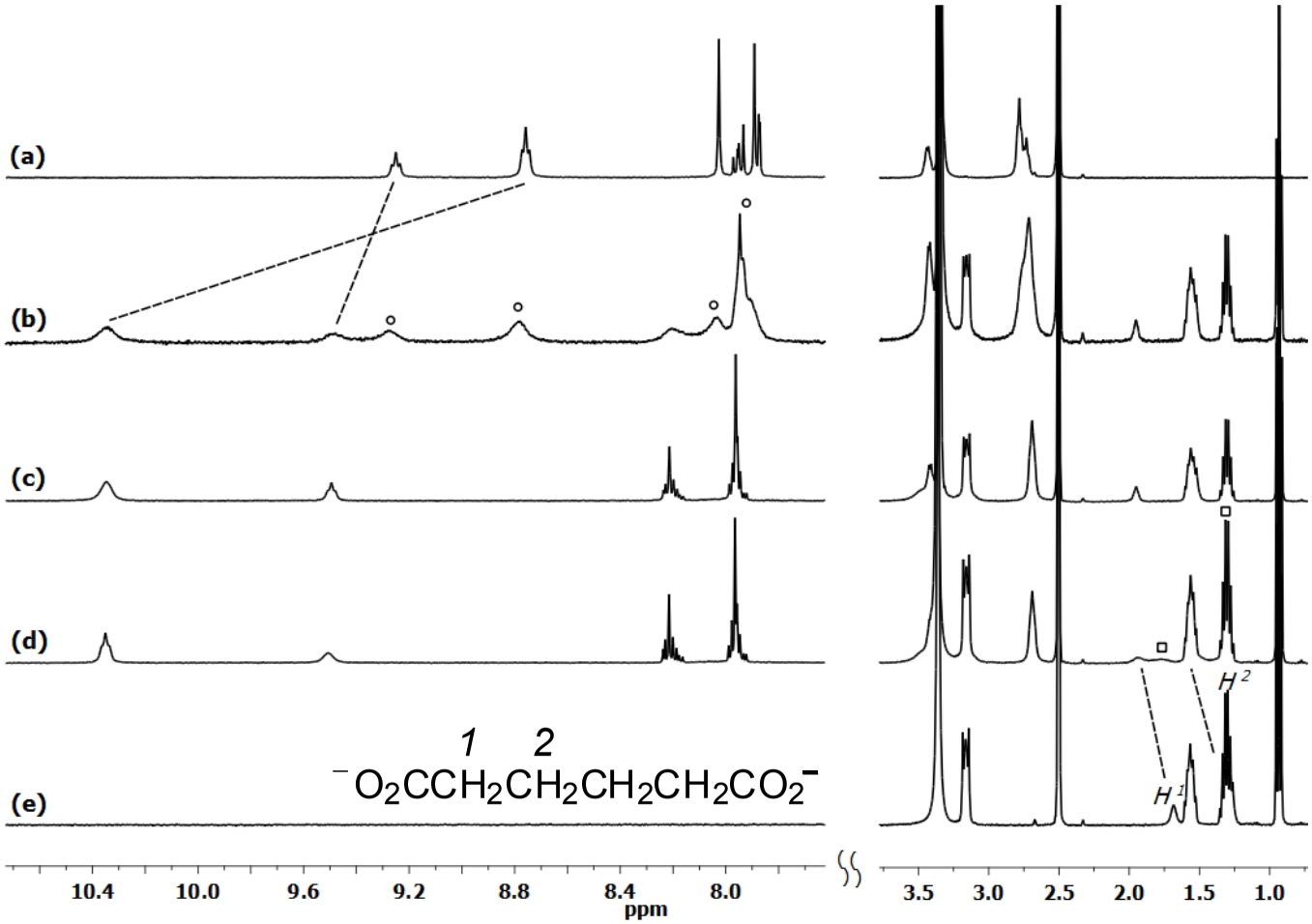

Figure S6. ^{1}H NMR spectra of **1** in DMSO-d_6 after adding adipate in different ratios (**1**/adipate): (a) 1:0, (b) 1:0.5, (c) 1:1, (d) 1:2 and (e) 0:1. "◦" and "▫" correspond to the signals of the unbound host and dicarboxylate respectively.

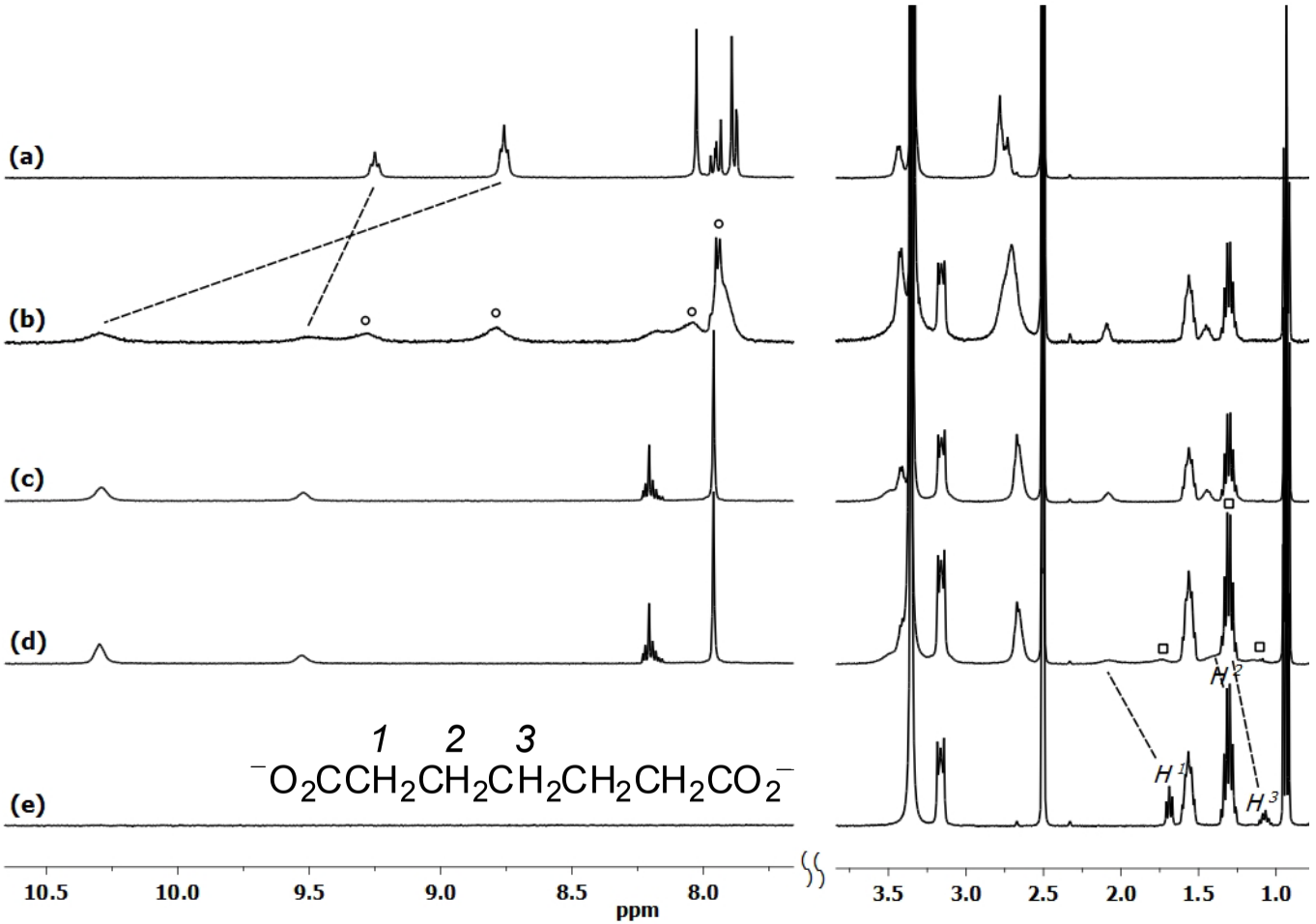

Figure S7. ^{1}H NMR spectra of **1** in DMSO-d_6 after adding pimelate in different ratios (**1**/pimelate): (a) 1:0, (b) 1:0.5, (c) 1:1, (d) 1:2 and (e) 0:1. "◦" and "▫" correspond to the signals of the unbound host and dicarboxylate respectively.

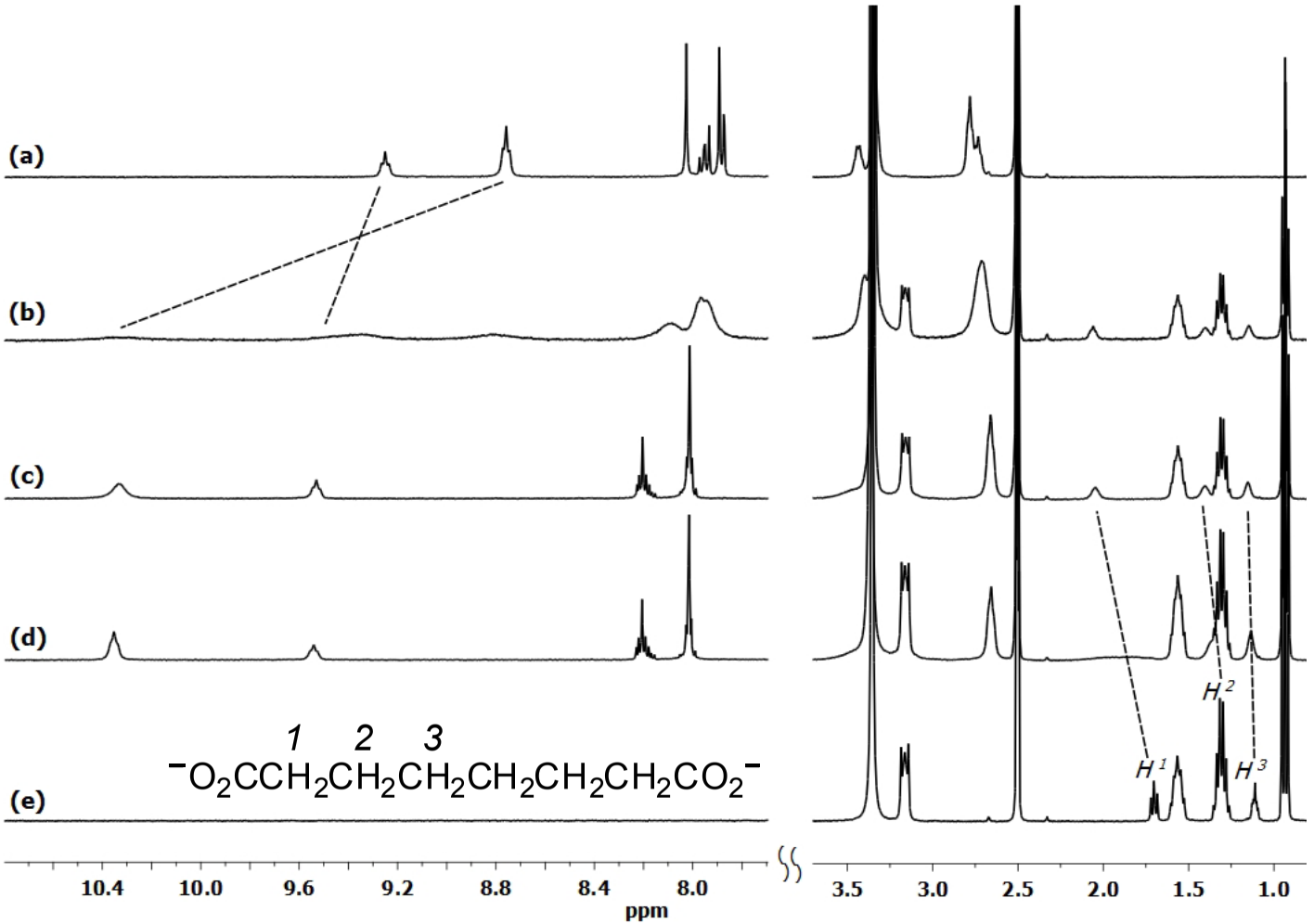

Figure S8. ^{1}H NMR spectra of **1** in DMSO-d_6 after adding suberate in different ratios (**1**/suberate): (a) 1:0, (b) 1:0.5, (c) 1:1, (d) 1:2 and (e) 0:1.

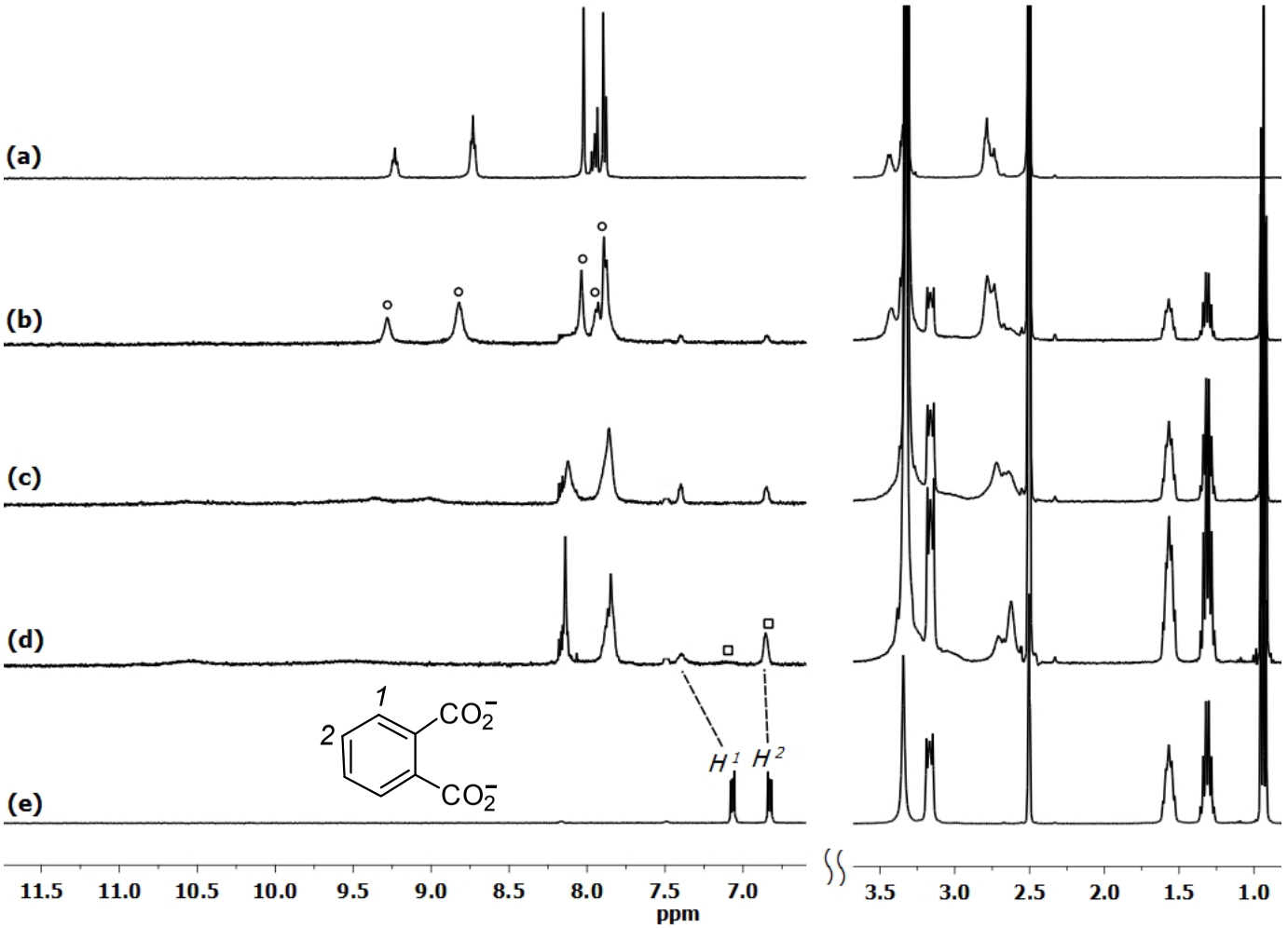

Figure S9. ^{1}H NMR spectra of **1** in DMSO-d_6 after adding phthalate in different ratios (**1**/phthalate): (a) 1:0, (b) 1:0.5, (c) 1:1, (d) 1:2 and (e) 0:1. "◦" and "▫" correspond to the signals of the unbound host and dicarboxylate respectively.

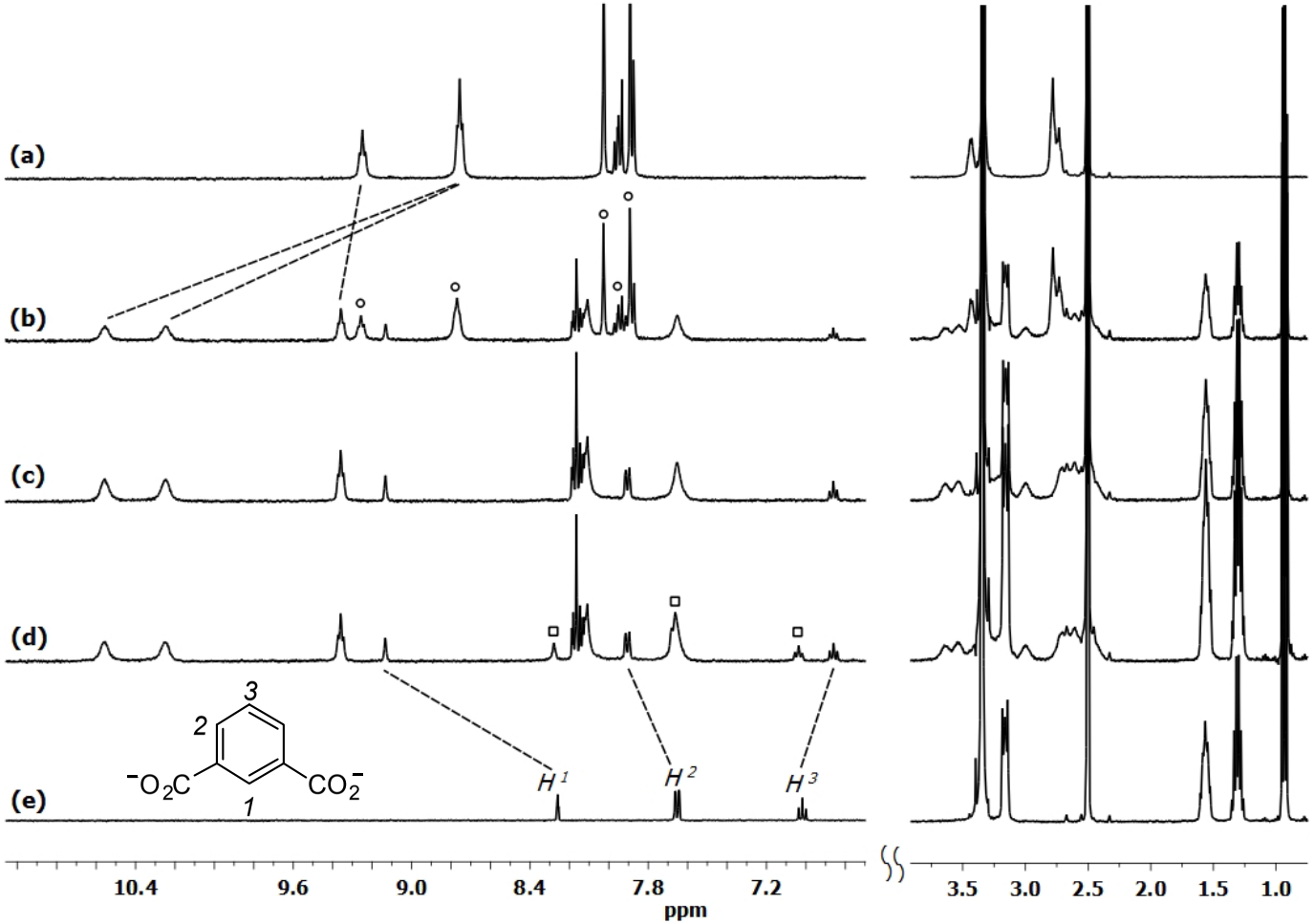

Figure S10. ^{1}H NMR spectra of **1** in DMSO-d_6 after adding isophthalate in different ratios (**1**/isophthalate): (a) 1:0, (b) 1:0.5, (c) 1:1, (d) 1:2 and (e) 0:1. "◦" and "▫" correspond to the signals of the unbound host and dicarboxylate respectively.

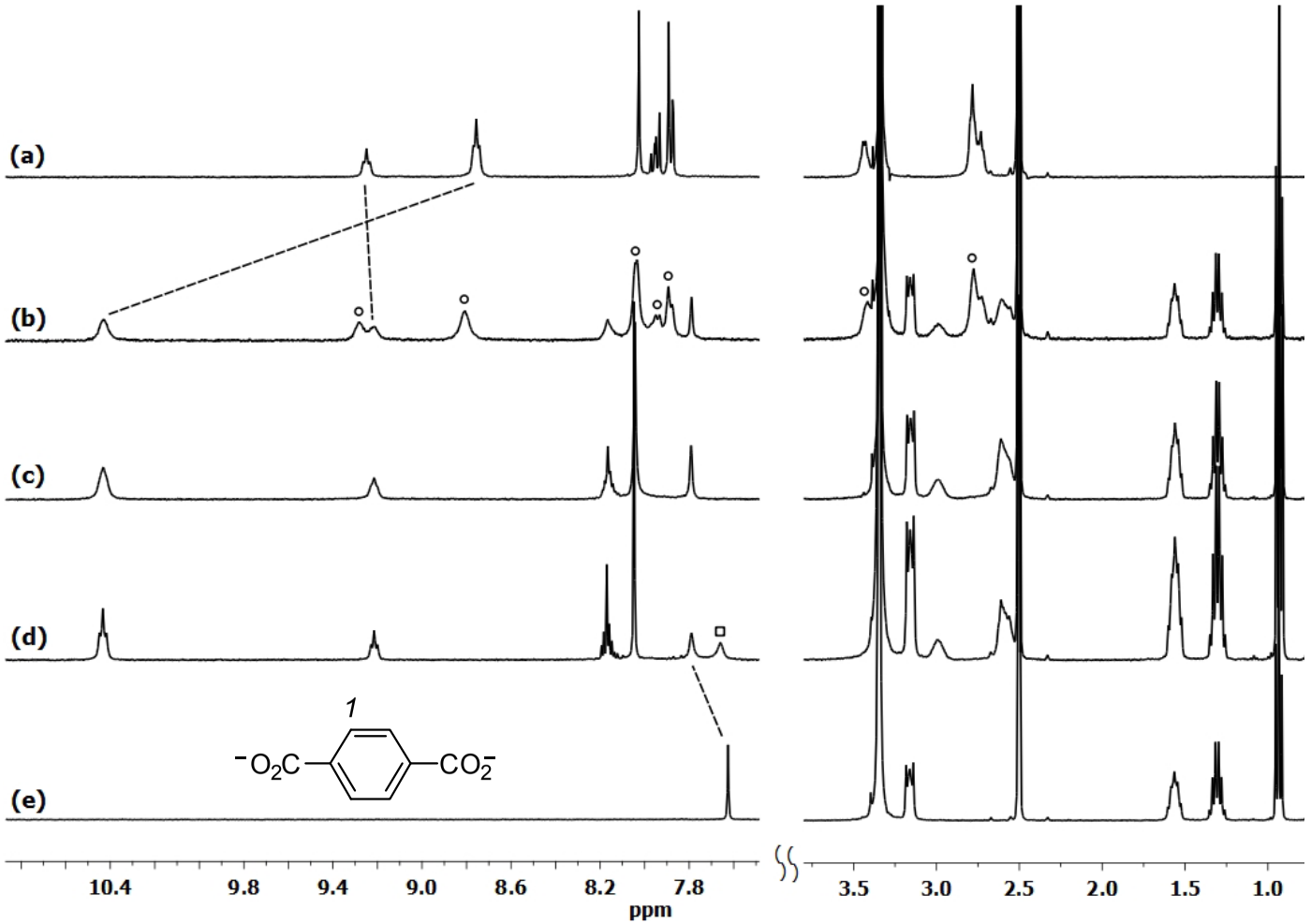

Figure S11. ^{1}H NMR spectra of **1** in DMSO-d_6 after adding terephthalate in different ratios (**1**/terephthalate): (a) 1:0, (b) 1:0.5, (c) 1:1, (d) 1:2 and (e) 0:1. "◦" and "▫" correspond to the signals of the unbound host and dicarboxylate respectively.

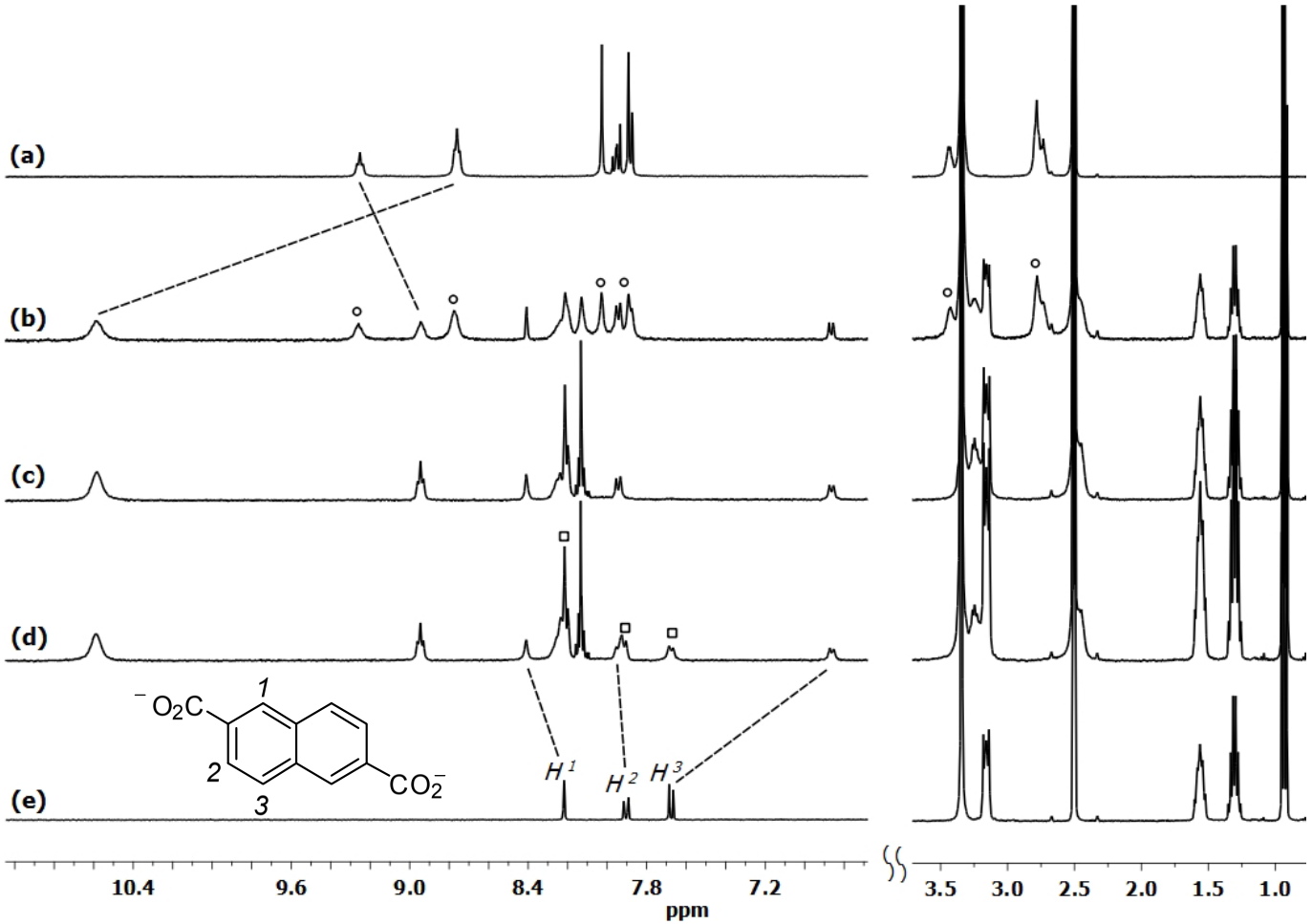

Figure S12. ^{1}H NMR spectra of **1** in DMSO-d_6 after adding 2,6-naphthalenedicarboxylate in different ratios (**1**/2,6-naphthalenedicarboxylate): (a) 1:0, (b) 1:0.5, (c) 1:1, (d) 1:2 and (e) 0:1. "◦" and "▫" correspond to the signals of the unbound host and dicarboxylate respectively.

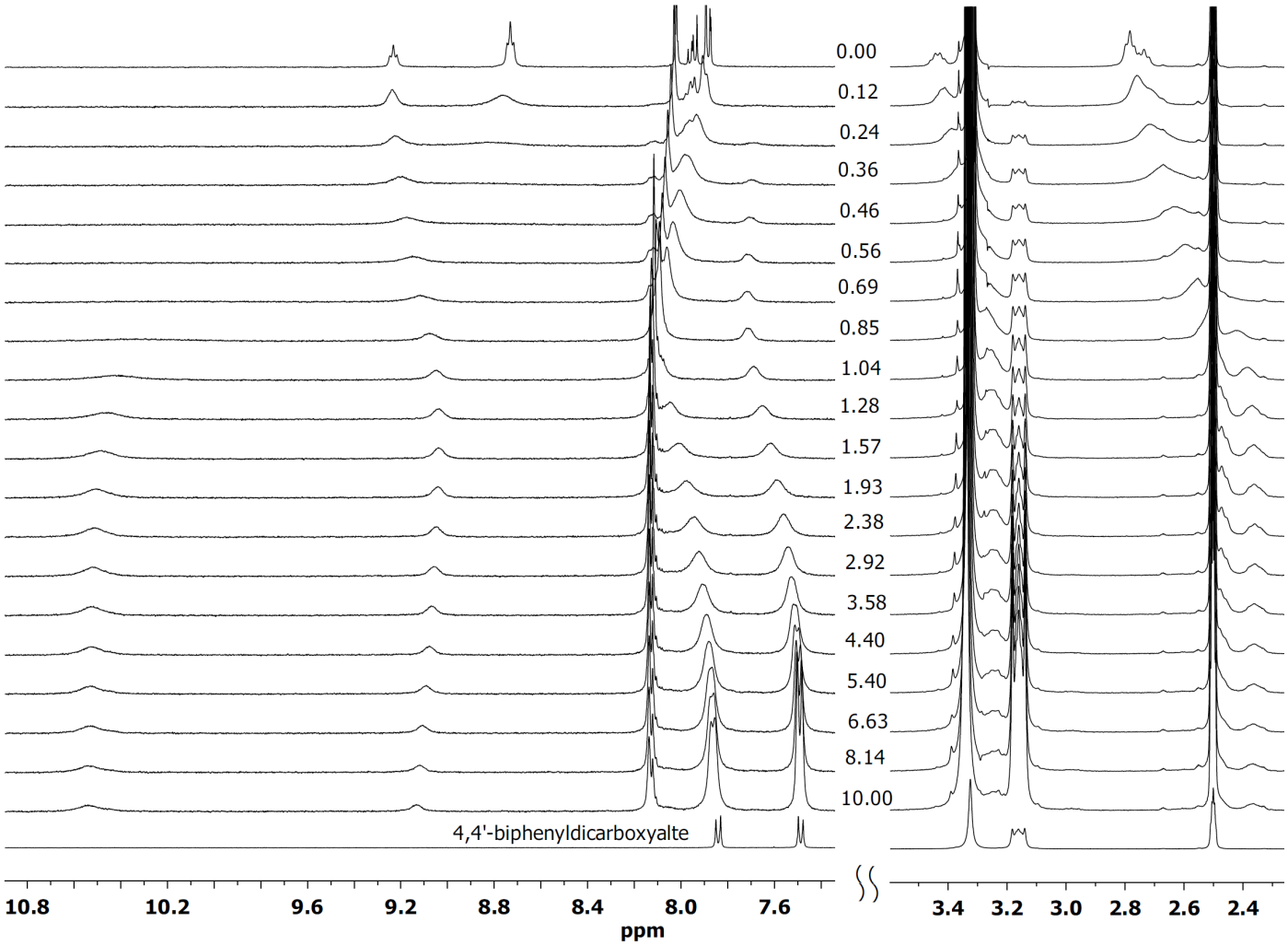

Figure S13. ^{1}H NMR titration spectra of **1** with 4,4′-biphenyldicarboxylate in DMSO-d_6. Numbers on the spectra indicate the equivalent amounts of 4,4'-biphenyldicarboxylate added.

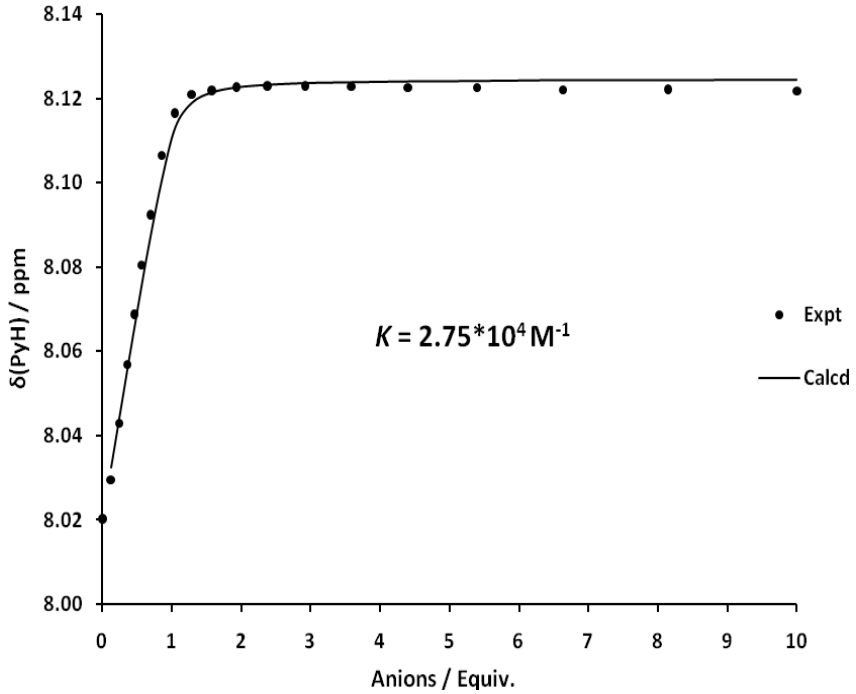

Figure S14. Plot of the chemical shift of one set *PyH* protons of **1** (2 mM) upon increasing the concentration of 4,4'-biphenyldicarboxylate in DMSO-d_6.

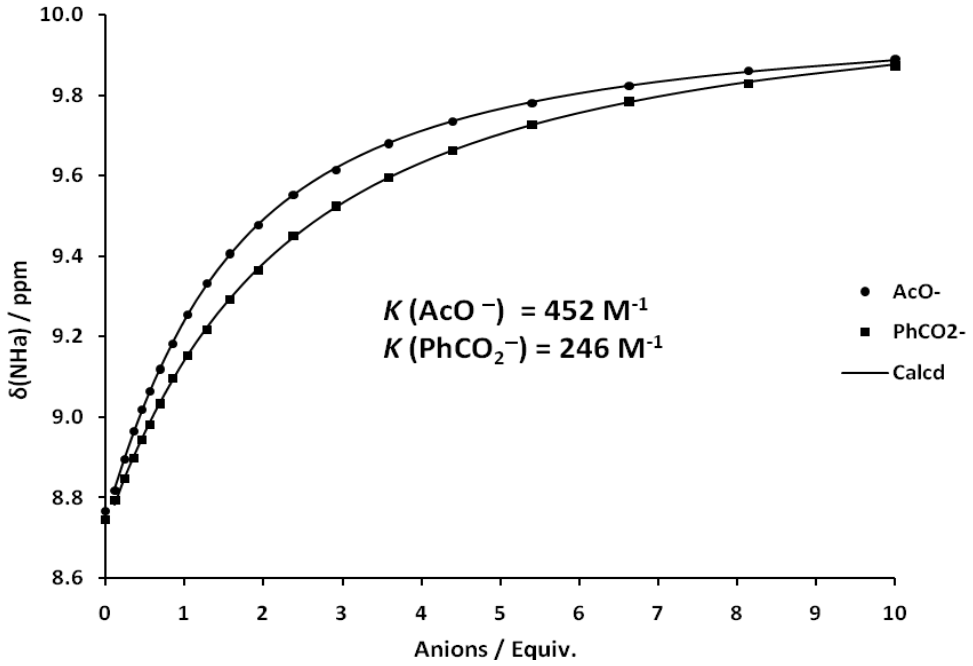

Figure S15. Plot of the NH^a chemical shift of **1** (2 mM) upon increasing the concentration of acetate and benzoate in DMSO-d_6.

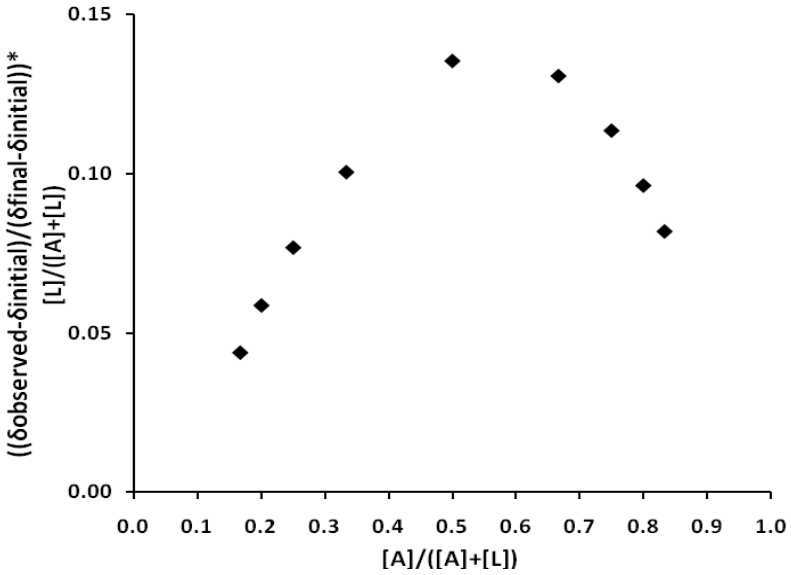

Figure S16. Job plot of **1** with acetate in DMSO-d_6. The total concentration of **1** and acetate was 2 mM.

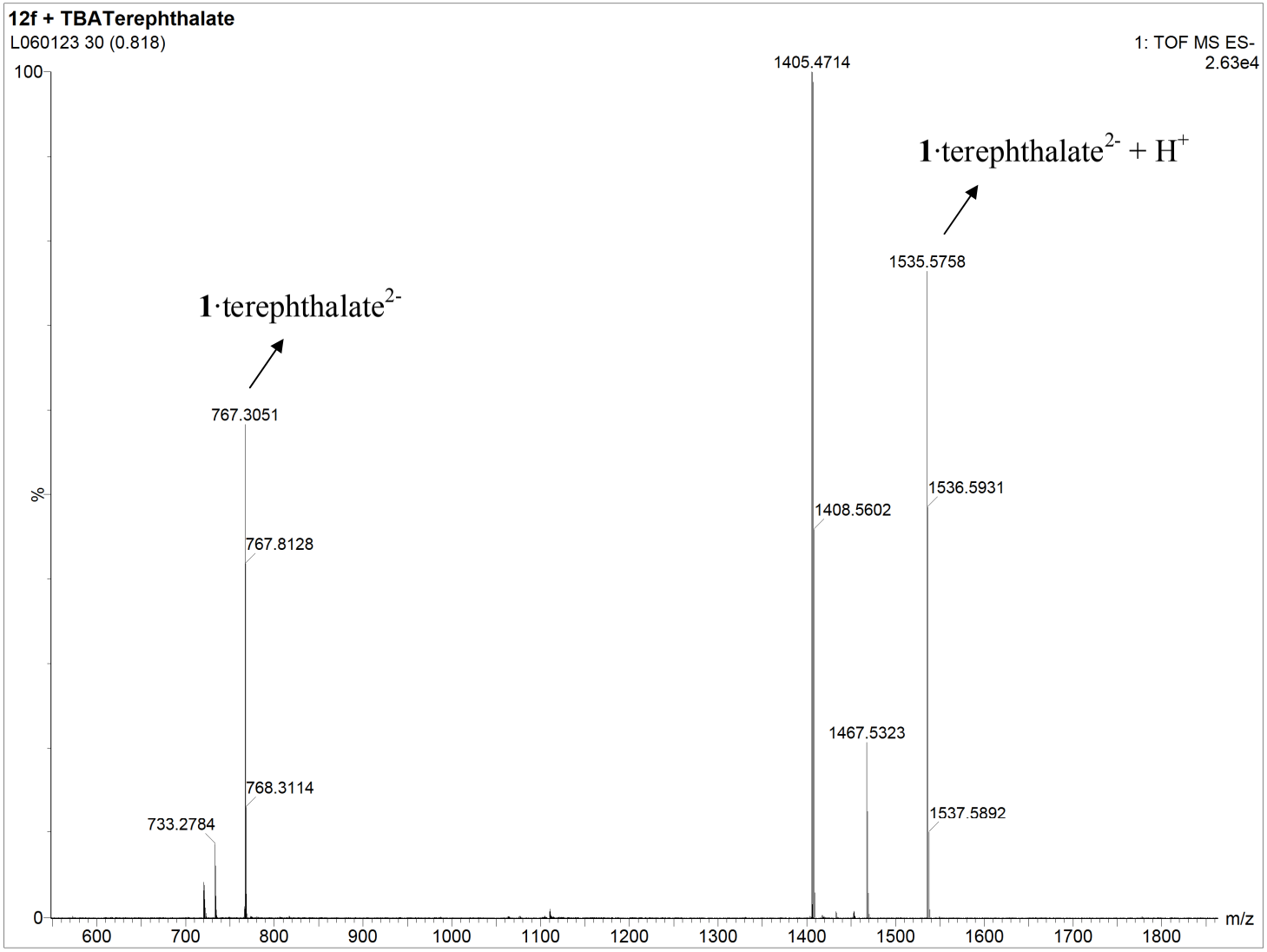

Figure S17. ESI-MS (negative) of the terephthalate complex of **1**.

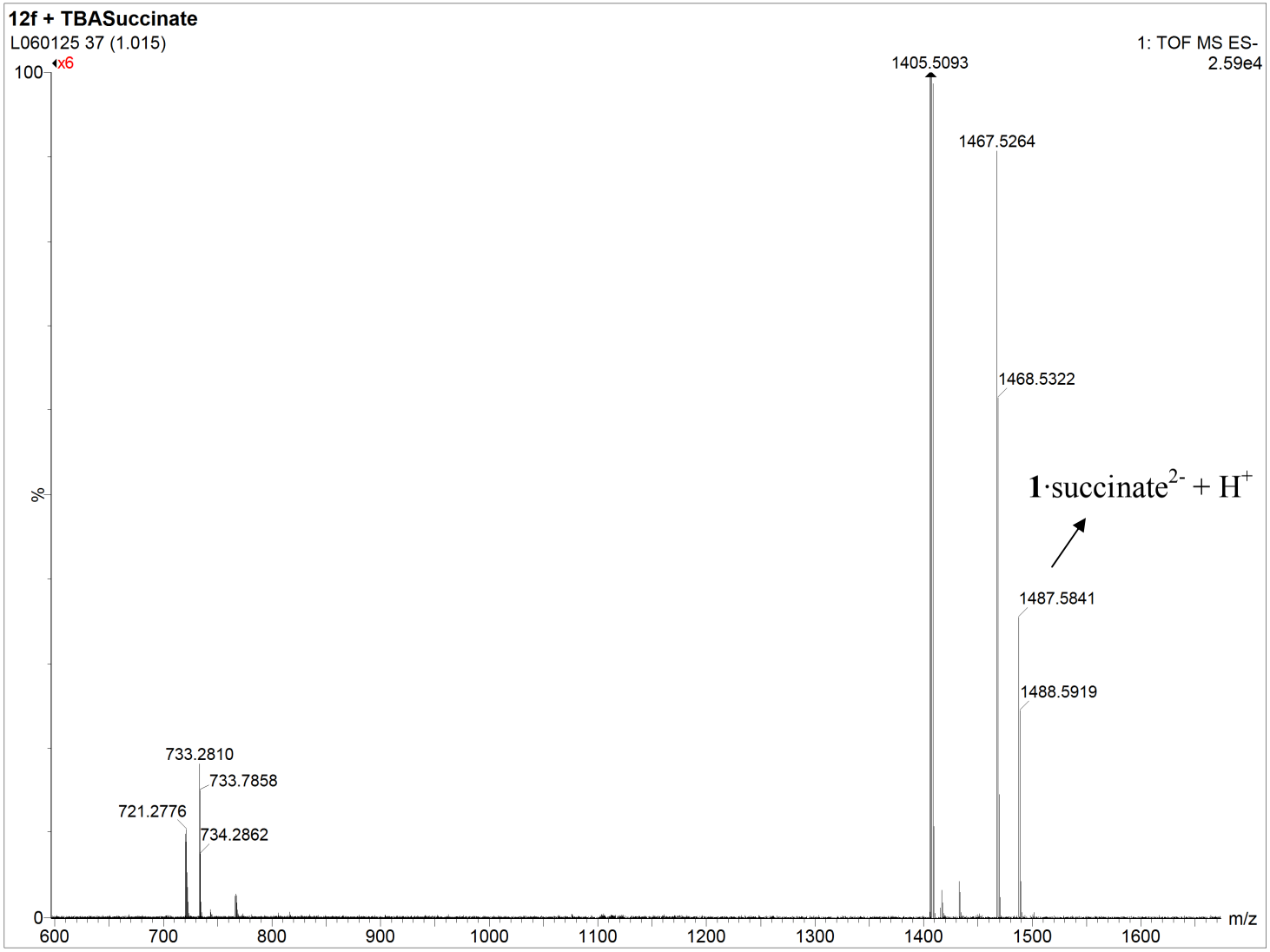

Figure S18. ESI-MS (negative) of the succinate complex of **1**.

Single crystal X-ray diffraction studies

Full hemispheres of diffracted intensities (1850 frames with an ω scan width of 0.30°) were measured for specimens of all three compounds using graphite-monochromated MoKα radiation (λ = 0.71073 Å) on a Bruker SMART APEX CCD Single Crystal Diffraction System. Frame counting times of 40 seconds (compounds **A** and **B**) or 10 seconds (compound **C**) were used for intensity data collection. X-rays were provided by a fine-focus sealed X-ray tube operated at 50kV and 35mA. Lattice constants were determined with the Bruker SAINT software package using peak centers for 7388(**A**), 5864(**B**) and 5301(**C**) reflections. The crystals of all three compounds used for data collection were either single-domain species. Integrated reflection intensities for all three compounds were produced using the Bruker program SAINT. Each data set was corrected empirically for variable absorption effects using equivalent reflections. The Bruker software package SHELXTL was used to solve each structure using "direct methods" techniques. All stages of weighted full-matrix least-squares refinement were conducted using F_o^2 data with the SHELXTL Version 6.10 software package.

The final structural model for each compound incorporated anisotropic thermal parameters for all nonhydrogen atoms except one disordered methylene carbon (C2s′) for a solvent molecule in **A** and three Cl and one C atom for the minor-occupancy (9%) site of a disordered $CHCl_3$ molecule in **C**; isotropic thermal parameters were incorporated for those atoms in **A** and **C** as well as all hydrogen atoms that could be located from difference Fouriers or placed at idealized positions in all three structures. Relevant data for the crystallographic studies of **A - C** are given in Table S2. The next four paragraphs describe the manner in which disorder was taken into account and the way hydrogen atoms were included in the structural models for these three compounds.

Two disordered ethanol solvent molecules of crystallization are present in **A**. The oxygen site (O1s) for the first of these sites appears to be occupied by a water oxygen atom part of the time and an ethanol oxygen the rest of the time. Disordered solvent carbon atom C1s was therefore assigned an occupancy factor of 0.50. The methylene carbon for the second ethanol molecule of crystallization in **A** is (65%/35%) disordered between two sites (C2s and C2s′). The third ethanol solvent molecule of crystallization in **A** is disordered with alternate (54%/46%) sites for the oxygen (O3s and O3s′) and alternate (70%/30%) sites for one of the carbons (C4s and C4s′). The occupancy factor for the oxygen of the third water molecule of crystallization was fixed at 0.50 since it is within 1.399 Å of its inversion-related site. Hydrogen atoms for the first two water molecules were located from a difference Fourier and included in the structural model as individual isotropic atoms whose positional parameters were allowed to vary in least-squares refinement cycles. Hydrogen atoms were not located for the (disordered) third water molecule.

There was no disorder in the structure for **B** and all hydrogen atoms were located from a difference Fourier and included in the structural model as individual isotropic atoms whose parameters were allowed to vary in least-squares refinement cycles.

The $CHCl_3$ molecule in **C** has two preferred orientations in the crystal. The major orientation is occupied 91% of the time and the minor is occupied 9% of the time. Nonhydrogen

atoms for the minor orientation of this molecule were refined with isotropic thermal parameters and restrained to have bond lengths and angles close to that of the major orientation. Hydrogen atoms for the first water molecule of crystallization were located from a difference Fourier and included in the structural model as individual isotropic atoms whose parameters were allowed to vary in least-squares refinement cycles. The occupancy factor for the oxygen of the second water molecule of crystallization (O2w) was fixed at 0.50 since it is within 1.301 Å of its inversion-related site. Hydrogen atoms were not located for this disordered water molecule.

The remaining hydrogen atoms bonded to carbon in **A** and **C** were included in their structural models as idealized atoms (assuming sp^2- or sp^3-hybridization of the carbon atoms and C-H bond lengths of 0.95 – 1.00 Å). Amide hydrogen atoms in **A** and **C** were included in the structural models as idealized atoms (assuming sp^2- hybridization of the nitrogen atoms and a N-H bond length of 0.88 Å). The isotropic thermal parameters of all hydrogen atoms whose thermal parameters were not refined were fixed at values 1.2 (nonmethyl) or 1.5 (methyl) times the equivalent isotropic thermal parameter of the nitrogen, oxygen or carbon atom to which they are covalently bonded.

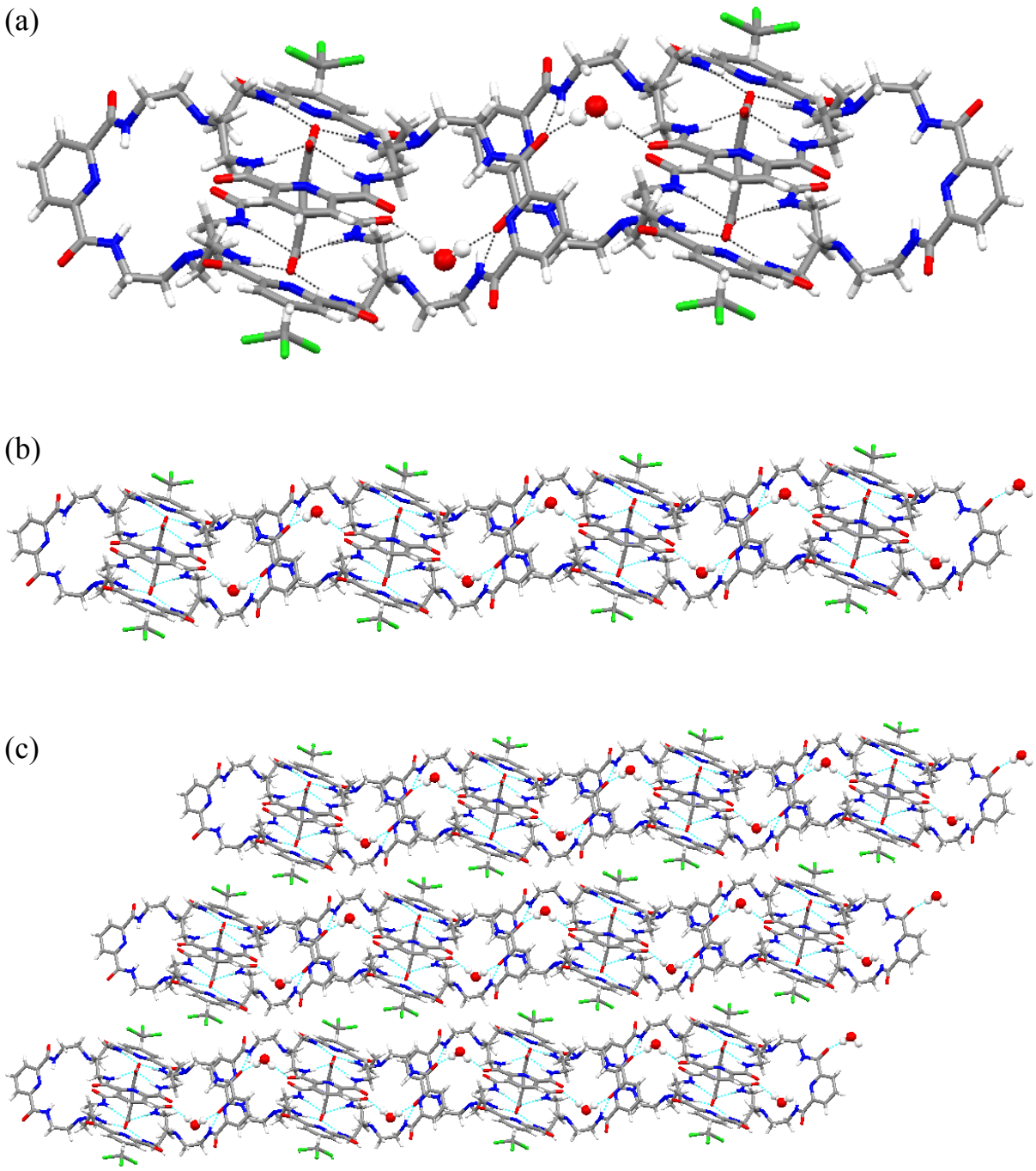

Figure S19. Assembly motif formed by water molecule H-bond link to a neighboring host in the succinate complex with **1**: dimeric (a), infinite 1D (b) and 2D (c) structures.

Table S2. Crystal Data and Structure Refinement for (**A**) **1**·5EtOH·6H_2O, (**B**) [*n*-Bu_4N]$_2$[**1**(terephthalate)]·4CH_3CN·6H_2O, (**C**) [Me_4N]$_2$[**1**(succinate)]·2$CHCl_3$·2CH_3CN·3H_2O.

	A	**B**	**C**
Empirical formula	C_{75} H_{86} N_{22} O_{23}	C_{114} H_{178} N_{28} O_{22}	C_{84} H_{118} Cl_6 N_{26} O_{19}
Formula weight	1663.66	2292.84	2008.74
Temperature	100(2) K	100(2) K	100(2) K
Wavelength	0.71073 Å	0.71073 Å	0.71073 Å
Crystal system	Monoclinic	Triclinic	Triclinic
Space group	C2/c – C_{2h}^6 (No. 15)	P-1 – C_i^1 (No. 2)	P-1 – C_i^1 (No. 2)
a	34.486(3) Å	13.477(4) Å	12.360(3) Å
b	11.340(1) Å	15.019(4) Å	14.699(4) Å
c	24.718(2) Å	17.319(5) Å	15.587(4) Å
a	90°	98.171(5)°	70.114(4)°
β	117.519(2)°	109.671(4)°	82.103(4)°
γ	90°	102.737(5)°	66.078(4)°
Volume	8573.0(11) Å^3	3129(2) Å^3	2434.2(11) Å^3
Z	4	1	1
Density (calculated)	1.289 Mg/m^3	1.217 Mg/m^3	1.370 Mg/m^3
Absorption coefficient	0.098 mm^{-1}	0.086 mm^{-1}	0.256 mm^{-1}
F(000)	3496	1234	1058
Crystal size	0.40 x 0.34 x 0.15 mm^3	0.46 x 0.21 x 0.09 mm^3	0.50 x 0.48 x 0.38 mm^3
Theta range	2.44 to 25.00°	2.32 to 27.50°	2.28 to 27.50°
Index ranges	$-40\le h\le 40$, $-13\le k\le 13$, $-29\le l\le 29$	$-17\le h\le 17$, $-19\le k\le 19$, $-22\le l\le 22$	$-16\le h\le 15$, $-18\le k\le 19$, $-20\le l\le 20$
Reflections collected	34276	28008	21116
Independent reflections	7548 [R_{int} = 0.057]	14109 [R_{int} = 0.043]	10954 [R_{int} = 0.035]
Completeness to θ_{max}	99.9 %	98.0 %	98.0 %
Absorption correction	Multi-scan	Multi-scan	Multi-scan
Max. and min. transmission	1.000 and 0.739	1.000 and 0.770	1.000 and 0.827
Refinement method	Full-matrix least-squares on F^2	Full-matrix least-squares on F^2	Full-matrix least-squares on F^2
Data / restraints / parameters	7548 / 0 / 586	14109 / 0 / 1095	10954 / 6 / 643
Goodness-of-fit on F^2	1.063	1.114	1.063
Final R indices [I>2σ(I)]	R_1 = 0.078, wR_2 = 0.219	R_1 = 0.067, wR_2 = 0.153	R_1 = 0.067, wR_2 = 0.175
R indices (all data)	R_1 = 0.112, wR_2 = 0.237	R_1 = 0.076, wR_2 = 0.158	R_1 = 0.074, wR_2 = 0.181
Largest diff. peak and hole	0.67 and -0.39 e$^-$/Å^3	0.56 and -0.43 e$^-$/Å^3	1.21 and -0.74 e$^-$/Å^3